

Characteristics and emission budget of carbonaceous species from post-harvest agricultural-waste burning in source region of the Indo-Gangetic Plain

By PRASHANT RAJPUT¹, MANMOHAN SARIN^{1*}, DEEPTI SHARMA² and DARSHAN SINGH², ¹Physical Research Laboratory, Ahmedabad 380 009, India; ²Punjabi University, Patiala 147 002, India

(Manuscript received 2 April 2013; in final form 9 December 2013)

ABSTRACT

Characteristics and emission budget of carbonaceous species from two distinct post-harvest agricultural-waste (paddy- and wheat-residue) burning emissions have been studied from a source region (Patiala: 30.2°N, 76.3°E; 250 m amsl) in the Indo-Gangetic Plain (IGP), Northern India. The PM_{2.5} mass concentration varies from 60 to 390 µg m⁻³ during paddy-residue burning (October–November) with dominant contribution from organic carbon (OC ≈ 33%), whereas contribution from elemental carbon (EC) centres at ~4%. Water-soluble organic carbon (WSOC) accounts for about 50% of OC. In contrast, mass concentration of PM_{2.5} during the period of wheat-residue burning (April–May) is significantly lower, varies from 18 to 123 µg m⁻³ and mass fractions of EC and OC are 7 and 26%, respectively. The diagnostic ratios of OC/EC (11 ± 2), WSOC/OC (0.52 ± 0.02), nss-K⁺/OC (0.06 ± 0.00) and ΣPAHs/EC (4.3 ± 0.7 mg/g) from paddy-residue burning emissions are significantly different than those from wheat-residue burning (OC/EC: 3.0 ± 0.4; WSOC/OC: 0.60 ± 0.03; nss-K⁺/OC: 0.14 ± 0.01 and ΣPAHs/EC: 1.3 ± 0.2 mg/g). The emission budget of OC, EC and ΣPAHs from post-harvest agricultural-waste burning in the IGP are estimated to be 505 ± 68 Gg/y, 59 ± 2 Gg/y and 182 ± 32 Mg/y, respectively. From a global perspective, crop-residue burning in Northern India contributes nearly 20% of both OC and EC to the total emission budget from the agricultural-waste burning.

Keywords: biomass burning emission, elemental carbon, organic carbon, water soluble organic carbon, polycyclic aromatic hydrocarbons, emission budget

1. Introduction

The hot-spots of atmospheric pollutants over the Indo-Gangetic Plain (IGP) and a thick layer of haze advecting towards the Bay of Bengal (BoB) during the wintertime have been documented through MODIS (MODerate resolution Imaging Spectroradiometer) imageries (Ramanathan et al., 2007). This has led to the suggestion on the impact of aerosols (particularly black carbon) and warming trend (heating rate: 0.15–0.30 K/decade) in Northern India (Ramanathan et al., 2007). The IGP occupies ~15% of the geographical area in south Asia, holds about 42% of the total population and accounts for 45% of food production (Gupta et al., 2004; Badarinath et al., 2006). The two major crops of paddy (rice) and wheat grown in the IGP contribute

nearly 85% of the entire production in south Asia. On a regional scale, 90–95% of rice and wheat crop rotation in India [total area under rice-wheat cultivation is ~20 million hectares (m ha)] are located in Punjab, Haryana and western part of Uttar Pradesh in the IGP. The burning of agricultural-waste in open fields for crop rotation is a common practice on annual and seasonal basis in north-west region of the IGP (Gupta et al., 2004; Badarinath et al., 2006; Punia et al., 2008).

The large-scale biomass burning emission in the IGP addresses the issue of contribution from secondary organic aerosol (SOA) and potential loss of atmospheric chemical constituents (O₃, NO_x and OH radical) via chemical reactions (Rengarajan et al., 2007; Rajput et al., 2011b; Ram and Sarin, 2011). During the wintertime (December–February), emissions from bio-fuel burning and fossil-fuel combustion sources are trapped in the lower atmosphere due to shallow planetary boundary layer associated

*Corresponding author.
email: sarin@prl.res.in

with fog-haze conditions in the IGP (Rengarajan et al., 2007; Rajput et al., 2011b; Ram et al., 2012). It is relevant to state that the post-harvest paddy-residue burning emissions can have a significant impact during the wintertime on the aerosol composition over Northern India. In this context, we present extensive data set on the characterisation of two major crop-residue (paddy- and wheat-residue) burning emissions in the IGP. The emission budget of organic and elemental carbon (OC, EC) and polycyclic aromatic hydrocarbon contributes significantly to the global emission scenario from agricultural-waste burning. Furthermore, we have also assessed the spatial variability in OC/EC ratio (as high as 6–10) as a characteristic feature of carbonaceous aerosols from different geographical locations during the wintertime in the IGP.

2. Methodology

2.1. Sampling site description

The large-scale biomass burning emission in Northern India (mainly in Punjab, Haryana and western Uttar Pradesh; $2^\circ \times 2^\circ = 48400$ sq km; Fig. 1), extending from north to the north-western part of the IGP, is a common practice followed by farmers on annual and seasonal basis. The post-harvest paddy-residue burning during October–November and wheat-residue burning during April–May are conspicuous features in the IGP. The intermediate period from December to February (wintertime) experiences fog

formation, a manifestation of shallower planetary boundary layer, emissions from bio-fuel burning and fossil-fuel combustion sources and moisture from western disturbances. In order to assess the chemical characteristics of ambient aerosols from these emission sources, samples of $PM_{2.5}$ (particulate matter with aerodynamic diameter $\leq 2.5 \mu\text{m}$) were collected from a sampling site at Patiala [30.2°N , 76.3°E ; 250 m above mean sea level (amsl)], where nearly 84% of the land area is under cultivation (Badarinath et al., 2006). During the period of SW-monsoon (June–September), frequent wet precipitation events amounting to 80–90% of the total annual precipitation (~ 1000 mm) wash out ambient aerosols. After monsoon, aerosol composition at the sampling site (upwind of the major population and industrial pollution sources) is considered to be representative of emissions from open paddy- (October–November) and wheat-residue burning (April–May) (Rajput et al., 2011b).

2.2. Analytical methods

Aerosol samples were collected using a high-volume sampler (flow rate: $1.2 \text{ m}^3 \text{ minutes}^{-1}$) by filtering ambient air through the pre-combusted (at 350°C for ~ 6 h) tisuquartz filters (PALLFLEX™, 2500QAT-UP, $20 \text{ cm} \times 25 \text{ cm}$). A total of 59 $PM_{2.5}$ samples were collected during paddy-residue burning emissions (October–November in 2008 and 2010), of which initial 33 samples were integrated for ~ 24 h each (in the first-campaign in 2008) and the remaining 26 samples

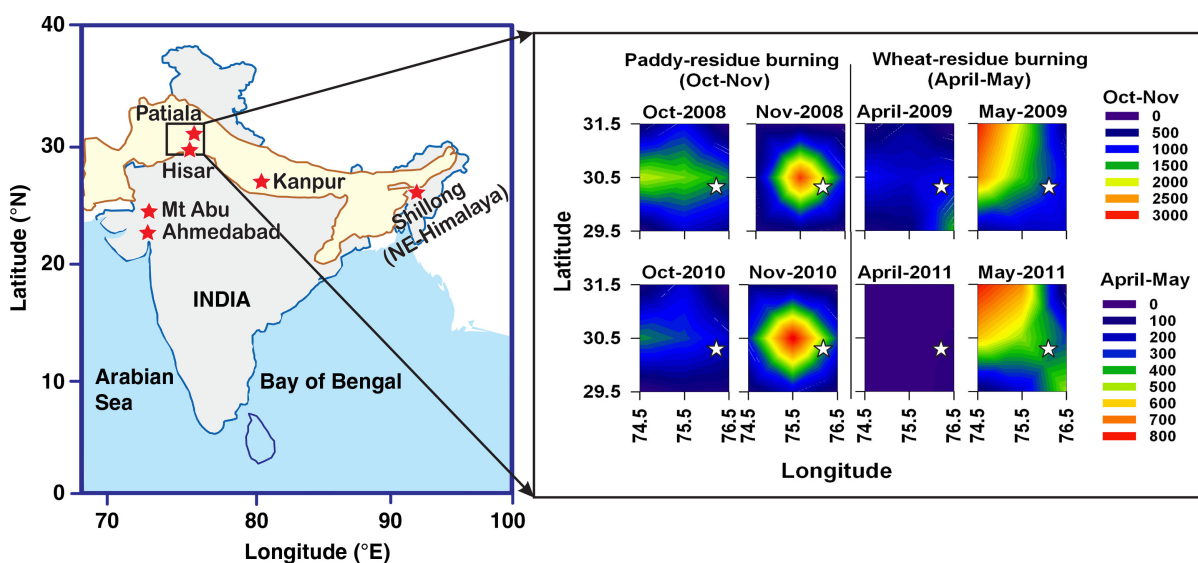


Fig. 1. Map of study locations: Patiala, Hisar and Kanpur in the Indo-Gangetic Plain (shown as yellow shaded area), at Barapani near Shillong in NE-Himalaya and at Ahmedabad and Mt Abu in semi-arid western India. MODIS derived fire-counts (plotted on the right) during the paddy- and wheat-residue burning period in the source region; sampling site at Patiala (shown by open star) is located downwind of major field-fires.

Table 1. Concentrations of carbonaceous species and characteristic ratios ($\text{Av} \pm \text{sd}$ given in parenthesis) from biomass burning emissions and fossil-fuel combustion in the Indo-Gangetic Plain (IGP)

Aerosol species	Paddy-residue burning (Oct–Nov; $n = 59$)	Wheat-residue burning (April–May; $n = 31$)	Difference ^a (two-tailed t -test)	Fossil-fuel and bio-fuel emissions (Dec–March; $n = 51$)
PM _{2.5} ($\mu\text{g m}^{-3}$)	60–391 (195 ± 87)	18–123 (50 ± 23)		19–244 (124 ± 58)
OC/PM _{2.5} (%)	21–50 (33 ± 7)	19–36 (26 ± 5)	S ($t = 4.9$)	12–31 (22 ± 4)
EC/PM _{2.5} (%)	2–6 (3.5 ± 1.1)	4–12 (6.9 ± 2.5)	S ($t = 9.0$)	2–9 (4.6 ± 1.8)
OC/EC ^b	4–26 (10.6 ± 1.6)	2.0–6.5 (3.0 ± 0.4)	S ($t = 26$)	1.9–10.1 (4.2 ± 0.8)
EC/TC ^b	0.04–0.18 (0.04 ± 0.00)	0.13–0.33 (0.19 ± 0.02)	S ($t = 58$)	0.09–0.35 (0.15 ± 0.01)
WSOC/OC ^b	0.41–0.91 (0.52 ± 0.02)	0.43–0.79 (0.60 ± 0.03)	S ($t = 15$)	0.45–0.86 (0.62 ± 0.03)
nss-K ⁺ /OC ^b	0.03–0.16 (0.06 ± 0.01)	0.04–0.15 (0.14 ± 0.01)	S ($t = 62$)	0.01–0.13 (0.06 ± 0.01)
ΣPAHs (ng m^{-3})	3.2–59.1 (27.1 ± 16.7)	1.2–17.0 (4.1 ± 3.5)		2.1–47.9 (16.9 ± 10.4)
ΣPAHs/OC (mg g^{-1}) ^b	0.07–0.96 (0.37 ± 0.04)	0.22–1.22 (0.30 ± 0.08)	S ($t = 5.5$)	0.12–0.82 (0.65 ± 0.07)
ΣPAHs/EC (mg g^{-1}) ^b	0.80–10.19 (4.25 ± 0.72)	0.69–2.35 (1.30 ± 0.20)	S ($t = 22.3$)	1.32–9.58 (3.41 ± 0.66)
PAHs isomer ratios				
3-ring				
ANTH/(ANTH + PHEN)	(0.19 ± 0.08)	(0.11 ± 0.04)	S ($t = 5.2$)	(0.15 ± 0.05)
4-ring				
FLA/(FLA + PYR)	(0.46 ± 0.02)	(0.50 ± 0.03)	S ($t = 7.5$)	(0.48 ± 0.02)
BaA/(BaA + CHRY + TRIPH)	(0.25 ± 0.05)	(0.24 ± 0.09)	IS ($t = 0.6$)	(0.28 ± 0.04)
5-ring				
BaP/(BaP + B[b,j,k]FLA)	(0.25 ± 0.05)	(0.26 ± 0.06)	IS ($t = 0.8$)	(0.27 ± 0.05)
6-ring				
IcdP/(IcdP + BghiP)	(0.49 ± 0.03)	(0.45 ± 0.05)	S ($t = 4.7$)	(0.50 ± 0.05)

^aComparison between paddy- and wheat-residue burning emissions.

^bCorrelation analysis. S (significant difference for $p < 0.05$) and IS (insignificant difference for $p > 0.05$).

ΣPAHs (PM_{2.5}-bound) include: NAPH, naphthalene; ACY, acenaphthylene; 2-BrNAPH, 2-bromonaphthalene; ACE, acenaphthene; FLU, fluorene; PHEN, phenanthrene; ANTH, anthracene; FLA, fluoranthene; PYR, pyrene; BaA, benzo[a]anthracene; CHRY + TRIPH, chrysene/triphenylene; B[b,j,k]FLA, benzo[b+j+k]fluoranthene; BaP, benzo[a]pyrene; IcdP, indeno[1,2,3-cd]pyrene; D[ah,ac]ANTH, dibenzo[a,h+a,c]anthracene; BghiP, benzo[g,h,i]perylene.

for 8–10 h each (daytime in the second-campaign in 2010), to collect the adequate aerosol mass on tissuquartz filters. However, during wheat-residue burning emissions (April–May in 2009 and 2011), all samples ($n = 31$) were collected during the daytime, integrating each sample for 8–10 h and so was the case during wintertime ($n = 51$; December 8–March 9 and December 10–March 11). The meteorological conditions (temperature, relative humidity and wind) are nearly same from year-to-year during the paddy-residue burning emissions (October–November, 2008 and 2010), and so is the case during wheat-residue burning emissions (April–May, 2009 and 2011). The meteorological parameters (temperature, relative humidity and wind) during

wintertime also do not exhibit inter-annual variability for the data set discussed in this study. The elemental carbon (EC) and organic carbon (OC) were measured on thermo-optical carbon analyser (Sunset Laboratory) using the NIOSH (National Institute for Occupational Safety and Health) protocol (Birch and Cary, 1996), water-soluble organic carbon (WSOC) on total OC analyser (Shimadzu; TOC 5000 A), water-soluble potassium on ion-chromatograph (Dionex[®]) and particulate-bound polycyclic aromatic hydrocarbons (here after referred as PAHs and in Table 1) on gas chromatograph coupled with a mass spectrometer (GC-MS, Agilent: 7890A/5975C) (Rengarajan et al., 2007; Rajput et al., 2011a, 2011b, 2013; Ram et al., 2012).

3. Results and discussion

3.1. Aerosol characteristics from post-harvest biomass burning emissions in the IGP

Post-harvest paddy-residue (with moisture content: 40–50%) is burnt in open fields (under ambient atmospheric conditions of 24–30°C temperature and 51–65% relative humidity), during October–November in the IGP (Gupta et al., 2004; Badarinath et al., 2006; Punia et al., 2008). The post-harvest wheat-residue (with moisture content: <5%) is burnt under ambient temperature ranging from 33 to 38°C at low relative humidity (34–41%), during April–May. The $PM_{2.5}$ mass concentration averages around $200 \mu\text{g m}^{-3}$ during the paddy-residue burning emission (Table 1; Fig. 2) and $\sim 50 \mu\text{g m}^{-3}$ during the wheat-residue burning emission. The average contributions of OC, EC and nss- K^+ to $PM_{2.5}$ from paddy-residue burning emission are 33, 3.5 and 2.4%, respectively (Fig. 2). From wheat-residue burning emission, the average contributions of OC, EC and nss- K^+ to $PM_{2.5}$ are 26, 7 and 2.4%, respectively.

The ΣPAHs (sum of 16 PAHs: 2- to 6-ring, reference is made to Table 1) average concentration from paddy-residue burning is 27.1 ng m^{-3} and from wheat-residue burning emission is 4.1 ng m^{-3} . The contribution of 4- to 6-ring PAHs ($\Sigma_{(4- \text{ to } 6-)}\text{PAHs}$) to the total PAHs (ΣPAHs) is $95 \pm 2\%$ for the two biomass burning emission sources. Further differences in the two biomass burning emission sources are assessed by the relative distribution of ring-wise PAHs with respect to the 6-ring PAHs. The 4-/6-ring and 5-/6-ring distributions also exhibit significant differences between the two biomass sources: relatively high ratios are recorded for the paddy-residue burning emission.

The $\Sigma\text{PAHs}/\text{OC}$ ratio of 0.4 mg g^{-1} from paddy-residue burning is relatively high (Table 1) than that from the wheat-residue burning emission (0.30 mg g^{-1}). Furthermore, the $\Sigma\text{PAHs}/\text{EC}$ ratio of 4.3 mg g^{-1} from paddy-residue burning is also higher (Table 1) than that from the wheat-residue burning emission (1.30 mg g^{-1}). The combustion of moist paddy-residue (with moisture content: 40–50%) during open biomass burning in October–November is responsible for higher contribution of OC to $PM_{2.5}$ and high-molecular weight PAHs (4- to 6-rings) in OC. In contrast, under dry weather conditions, the emissions from wheat-residue burning (with moisture content <5%) gives higher contribution of EC in $PM_{2.5}$ as compared to that from paddy-residue burning emission ($\text{EC}/PM_{2.5}$: 3.5%).

Based on linear regression analyses ($p < 0.0001$) among OC, EC, nss- K^+ and WSOC, the characteristic ratios of OC/EC , $\text{nss-}K^+/\text{OC}$ and WSOC/OC are constrained for the emissions from agricultural-residue burning (Table 1, Fig. 3). The OC/EC ratio of 10.6 for paddy-residue burning emission is significantly higher than that for the wheat-residue burning emission (3.0; Fig. 3a). The $\text{nss-}K^+/\text{OC}$ ratio of 0.06 for the paddy-residue burning emission is also different, lower by a factor of 2 than that from the wheat-residue burning emission (0.14; Fig. 3b). This is attributable to the high abundance of OC from paddy-residue burning emission. Furthermore, a major fraction of OC is found to be soluble in water from both the biomass burning emissions: the WSOC/OC ratio of 0.52 for paddy-residue is lower than that for the wheat-residue burning emission (0.60; Fig. 3c). In this context, an earlier study reports that the WSOC can have primary production from biomass burning emission as well as secondary formation pathway

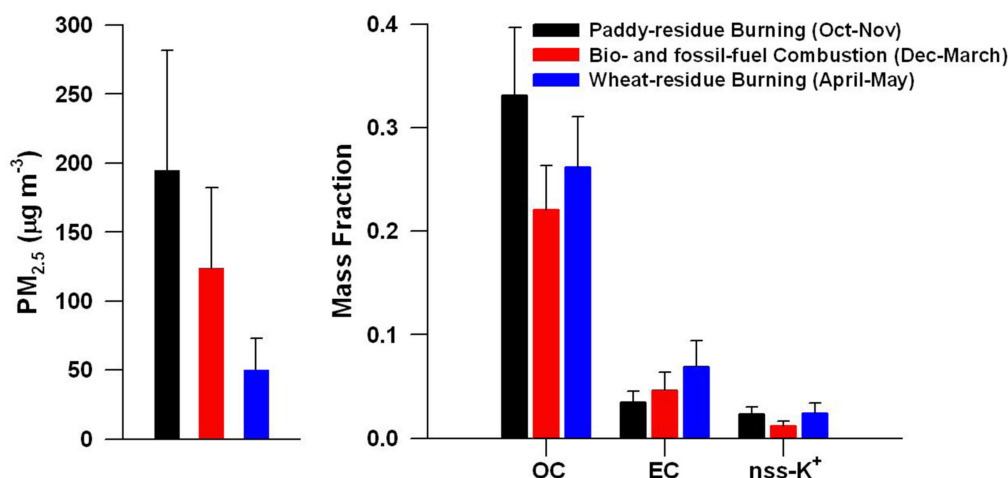


Fig. 2. Temporal variability in $PM_{2.5}$ and mass fractions of OC, EC and nss- K^+ associated with different emissions from source region (Patiala, Fig. 1) in the Indo-Gangetic Plain. The $\text{nss-}K^+ = K^+_{\text{aerosol}} - 0.037 * Na^+_{\text{aerosol}}$; where K^+ / Na^+ mass ratio of 0.037 is used for sea-salt contribution of K^+ (Keene et al., 1986).

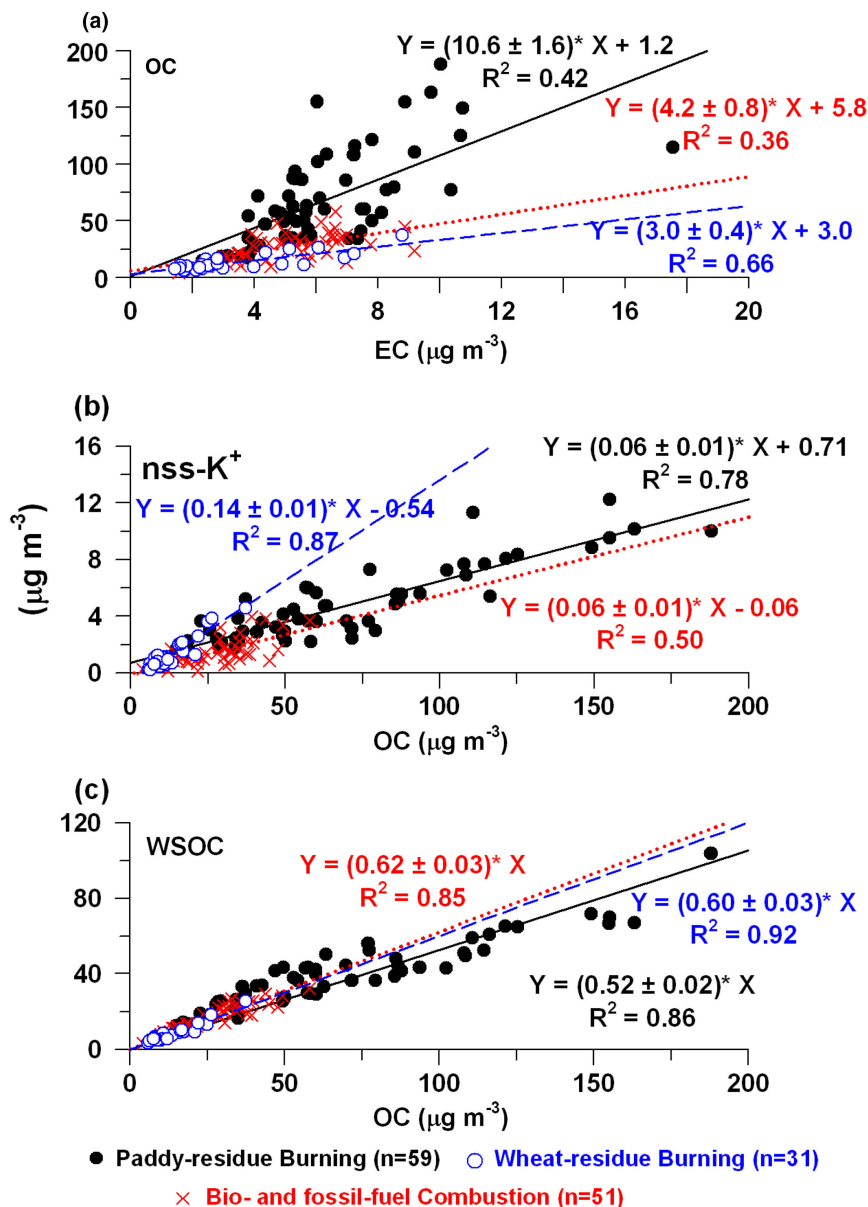


Fig. 3. Scatter plots of (a) EC vs. OC; (b) OC vs. non-sea-salt: nss-K⁺; and (c) OC vs. WSOC during different emissions in the IGP.

via photochemical reactions in the atmosphere (Mayol-Bracero et al., 2002). It is important to state here that a recent study from the Amazonian forest has suggested the significance of biogenic potassium to serving as a seed for SOA formation (Pöhlker et al., 2012). Thus, the SOA production can be favoured by their condensation onto K⁺ particles following the photochemical reactions of volatile organic compound (VOC) with atmospheric oxidants. In our context, it is likely possible that the biomass burning derived potassium could also serve as a seed for the SOA production. Relatively high abundances of nss-K⁺ and OC in PM_{2.5} from paddy-residue burning emission would facilitate higher contribution of secondary organic

carbon (SOC) than that from the wheat-residue burning (Fig. 3b; Table 1). Furthermore, during wintertime (December–March) the OC with EC and OC with nss-K⁺ suggests for the dominant impact from biomass burning emission in the IGP [OC/EC: 4.2; nss-K⁺/OC: 0.06]. The WSOC/OC ratio (0.62) in winter looks also similar to that observed from two distinct post-harvest biomass burning emissions (of paddy- and wheat-residue).

PAH isomer ratios for the fossil-fuel combustion, forest fires and bio-fuels burning emission are available in the literature (Kirton et al., 1991; Khalili et al., 1995; Masclet et al., 1995; Schauer et al., 2001; Sheesley et al., 2003; Khillare et al., 2005a, 2005b). However, the information

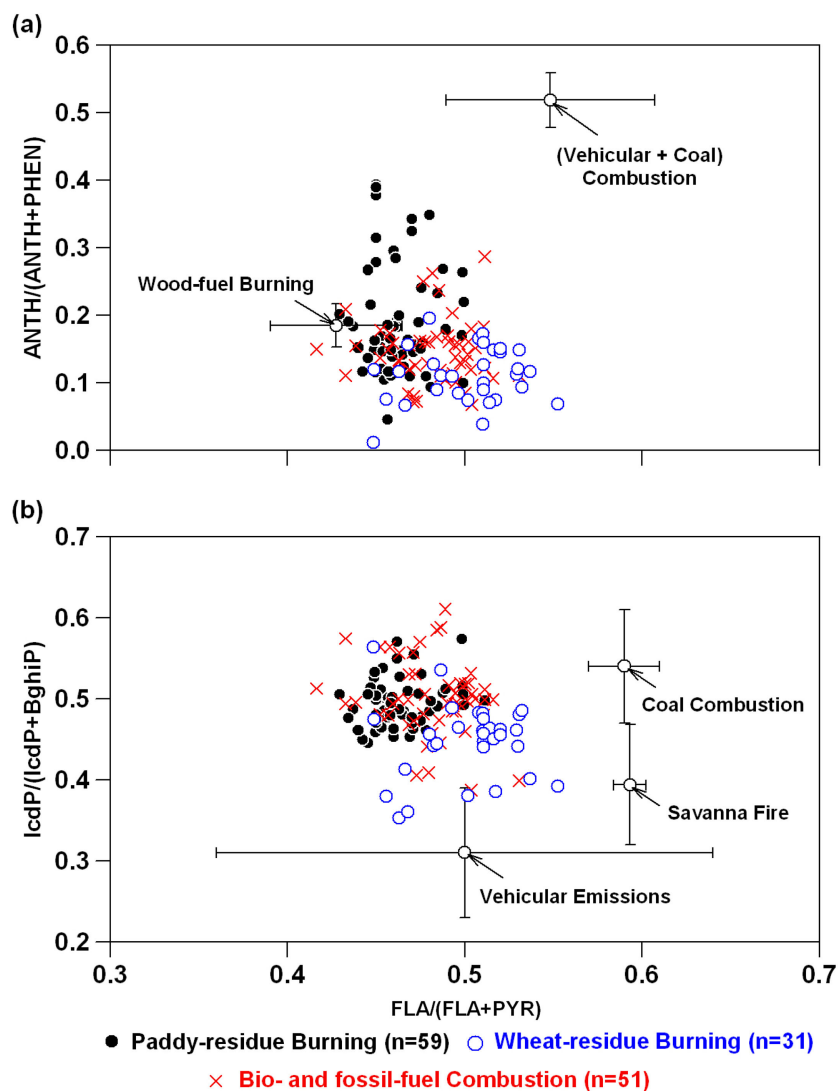


Fig. 4. Cross plots of PAH isomers showing distinct differences for the biomass burning emission vis-à-vis fossil-fuel combustion in the IGP: (a) FLA/(FLA + PYR; 4-ring on X-axis) vs. ANTH/(ANTH + PHEN; 3-ring on Y-axis); and (b) FLA/(FLA + PYR; 4-ring on X-axis) vs. IcdP/(IcdP + BghiP; 6-ring on Y-axis). Other data source: wood-fuel burning (Bari et al., 2009); (Vehicular + Coal) combustion (Sharma et al., 2008); vehicular emission (Khillare et al., 2005a, b; Rajput and Lakhani, 2008); coal combustion (Kirton et al., 1991; Khalili et al., 1995; Li et al., 2010); savanna fire (Masclat et al., 1995).

on PAH isomer ratios from the two potential sources of carbonaceous aerosols in the IGP, paddy- and wheat-residue burning (under ambient atmospheric conditions) is rather lacking in the literature (Rajput et al., 2011b). In this context, the present study serves to provide several PAH isomer ratios along with the major composition of carbonaceous species (EC, OC and WSOC) and nss-K⁺ in PM_{2.5} from paddy- and wheat-residue burning emission for statistically significant number of data set (Table 1). Employing the PAH isomers, ANTH/(ANTH + PHEN) and IcdP/(IcdP + BghiP) against FLA/(FLA + PYR) in the cross plots, we document a characteristic information for the post-harvest agricultural-waste burning emissions from

paddy- and wheat-residues (Fig. 4a and b; Table 1), distinctly different from the fossil-fuel combustion sources. The chemical characteristics of carbonaceous aerosols from biomass burning and fossil-fuel combustion sources in the IGP (from Patiala) during wintertime are summarised in Table 1 (for $n = 51$).

3.2. OC/EC ratio during wintertime (December–March) from different geographical locations in India

Earlier studies conducted in the IGP have reported on the concentrations of OC and EC in total suspended particulate matter (TSP; Table 2) during the wintertime

Table 2. Spatial distribution of OC/EC ratio in ambient aerosols from the Indo-Gangetic Plain (IGP) and different locations during wintertime (December–March)

Location	N	Concentration ($\mu\text{g m}^{-3}$)	OC	EC	OC/EC	
			%			
IGP						
Patiala	51	124 ± 58 (PM _{2.5})	22 ± 4	4.6 ± 1.8	4.2 ± 0.8	This study
Hisar	42	177 ± 64 (TSP)	17	2.1	8.5 ± 2.2	Rengarajan et al., 2007
Kanpur	17	141 ± 73 (TSP)	18	3.4	6.2 ± 3.7	Ram and Sarin, 2010
Allahabad	19	300 ± 90 (TSP)	16	2.1	8.1 ± 1.7	
Western India						
Ahmedabad	16	85 ± 37 (PM _{2.5})	33 ± 6	6 ± 1	6.1 ± 1.2	This study
Mt Abu	15	22 ± 9 (PM _{2.5})	10 ± 6	3.3 ± 1.6	3.0 ± 1	This study
Mumbai	4	128 ± 27 (PM ₁₀)	20	10	2.0 ± 0.3	Venkataraman et al., 2002
Southern India						
Chennai	29	(PM ₁₀) ^a			1.5 ± 0.5	Pavuluri et al., 2011
Himalaya						
NE-Himalaya	51	97 ± 50 (PM _{2.5})	36 ± 8	6 ± 3	6.8 ± 3.2	Rajput et al., 2013
NCO-P	28	(PM ₁₀) ^a			11 ± 2	Decesari et al., 2010
Manora peak	38	66 ± 18 (TSP)	16	3	6.3 ± 2.2	Ram et al., 2010
Ocean						
Northern-BoB	31	38 ± 20 (PM _{2.5})	16	5	3	Srinivas et al., 2011
Southern-BoB		22.3 ± 9.9 (PM _{2.5})	12	5	2.2	

^aPM₁₀ concentration is not reported (NR).

TSP refers to total suspended particulate matter.

(December–March) (Rengarajan et al., 2007; Ram and Sarin, 2010). The spatial variability in average concentration of TSP was reported to be ~100–400 during the wintertime in the IGP. The average mass fractions of OC and EC are nearly identical varying from ~16–18 and 2–4%, respectively, at study locations (Table 2). Based on the aerosol composition analysis from December 2008 to March 2009 and December 2010 to March 2011 at Patiala in the IGP (this study), we find PM_{2.5} concentrations varying from 19 to 244 (124 ± 58) $\mu\text{g m}^{-3}$ (Tables 1 and 2), quite similar to TSP from other locations in the IGP. The mass fractions of OC (22 ± 4%) and EC (4.6 ± 1.8%) in PM_{2.5} at Patiala are also quite similar to that in TSP over other locations (Hisar, Kanpur and Allahabad) during the wintertime. Thus, contribution of fine-mode aerosols (aerodynamic diameter $\leq 2.5 \mu\text{m}$) to TSP is dominant during the wintertime. The major source of particulate matter during the wintertime in the IGP is attributed to emissions from bio-fuel burning and fossil-fuel combustion sources (Rengarajan et al., 2007; Ram and Sarin, 2010; Rajput et al., 2011b).

Furthermore, downwind transport of pollutants from IGP along the foot-hills of NE-Himalaya, during the wintertime, has been documented by a recent study from NE-Himalaya [Barapani: 25.7°N, 91.9°E; 1064 m amsl; $n = 51$, January–March 2009 and 2010], wherein PM_{2.5}

concentration varies from 39 to 348 (Av: 97 ± 50) $\mu\text{g m}^{-3}$; of which OC and EC contributes 36 ± 8 and 6 ± 3%, respectively (Rajput et al., 2013). The OC/EC ratio ~7.0 from the foot-hills of NE-Himalaya is similar to that observed from several locations in the IGP. In contrast, over northern Bay of Bengal (N-BoB: ~10–20°N latitude; $n = 31$) the PM_{2.5} concentration in the marine atmospheric boundary layer (MABL) varies from 13.2 to 76.7 (38 ± 20) $\mu\text{g m}^{-3}$; with contributions from OC and EC as 16 and 5%, respectively (Srinivas et al., 2011). The PM_{2.5} concentration over the southern BoB (S-BoB: ~2–10°N latitude) varies from 2.0 to 35.3 (22.3 ± 9.9) $\mu\text{g m}^{-3}$; with contributions from OC and EC as 12 and 5%, respectively. Thus, OC mass fraction decreases, whereas EC contribution remains constant as a function of distance from the source region (with north-south gradient over open ocean). This is attributable to the preferential removal of OC (residing in coarse fraction) compared to EC (in fine fraction) in the MABL over the BoB. A systematic decrease in OC/EC ratio has been also observed over the Pacific in the outflow from East Asia (Lim et al., 2003). They attributed the decrease in OC/EC ratio to relatively longer atmospheric life-time of EC than OC in the MABL.

In order to assess the spatial distribution of carbonaceous aerosol in terms of OC/EC ratio from different geographical locations over India, aerosol sampling during

wintertime from two additional sites, at Ahmedabad [23.03°N, 72.65°E; 49 m amsl; $n=16$, 1 December 2009–28 January 2010] and Mt Abu [24.6°N, 72.7°E; 1680 m amsl; $n=15$, 12 February–17 March 2010] in semi-arid region of western India, has been conducted in this study. The $PM_{2.5}$ concentration varied from 32 to 161 ($Av \pm sd$: 85 ± 37) $\mu g m^{-3}$, of which $33 \pm 6\%$ is OC and $6 \pm 1\%$ is EC at Ahmedabad. The $PM_{2.5}$ concentration varied from 10 to 38 (22 ± 9) $\mu g m^{-3}$, of which $10 \pm 6\%$ is OC and $3.3 \pm 1.6\%$ is EC at Mt Abu. It is relevant to state that during wintertime, prevailing NE-winds favour the long-range transport of pollutants from the IGP to western India. Thus, aerosols over Ahmedabad represent regional characteristics as well as components from long-range transport. However, the other site in western India at Mt Abu (1680 m amsl) is by-and-large impacted by the long-range transport.

The OC/EC average ratio as high as ~ 6 – 10 in the upwind locations in the IGP (Table 2) is attributable to the dominance of biomass burning emission sources and photochemical reactions (Rengarajan et al., 2007; Ram and Sarin, 2010; Rajput et al., 2011a). A similar OC/EC ratio of ~ 6 from Manora Peak and ~ 10 in aerosols from the southern slope of higher Himalaya (National Climate Observatory-Pyramid; NCO-P sampling station) have been also attributed earlier to the dominance of biomass burning emissions and/or contributions from SOA (Decesari et al., 2010; Ram et al., 2010). Furthermore, a similar OC/EC ratio from a semi-arid location at Ahmedabad (~ 6) is observed during wintertime. In contrast, at other places in India (Mumbai and Chennai), the OC/EC ratio is ~ 2 – 3 (Venkataraman et al., 2002; Pavuluri et al., 2011). However, the OC/EC ratio in winter over the BoB has been reported to be > 2 (Srinivas et al., 2011). Thus, we integrate the present-day wintertime (December–March) scenario on significant variability in the chemical characteristics of

carbonaceous aerosols in terms of the OC/EC ratio from the IGP and those over different environmental regions in and around the country.

3.3. Emission budget of carbonaceous species from paddy- and wheat-residue burning in the IGP

The emission of carbonaceous species (EC, OC and $\Sigma PAHs$) from the paddy- and wheat-residue burning in the IGP is estimated using the following equation:

$$Emission (Gg/y) = EF (g/kg) * FL (kg/km^2) * AB (km^2/y) * 10^{-9} \quad (1)$$

Here, ‘EF’ is abbreviated for emission factor; ‘FL’ for fuel load over the agricultural fields and ‘AB’ for annual area burnt in the IGP (Table 3). A factor of 10^{-9} is multiplied to convert gram-emissions into Giga-grams (Gg).

In this study, the EF for carbonaceous species (EC, OC and $\Sigma PAHs$) from post-harvest paddy- and wheat-residue burning is suitably adopted from recent studies (Hays et al., 2005; Kanokkanjana et al., 2011). We have taken into consideration the differences in the OC/ $PM_{2.5}$ and EC/ $PM_{2.5}$ ratios for the biomass burning under ambient atmospheric conditions and those based on chamber experiments in order to assess the emission factors (Hays et al., 2005; Kanokkanjana et al., 2011). In case of paddy-residue burning emissions, the average mass fraction of (OC+EC)/ $PM_{2.5}$ is $36.5 \pm 7.1\%$ (this study). This mass fraction is in close agreement with that reported ($38 \pm 2\%$) in a recent study (Kanokkanjana et al., 2011) for moist combustion of paddy-residue from irrigated fields. Therefore, we have adopted the EF of EC as 0.72 ± 0.03 g/kg reported by (Kanokkanjana et al., 2011). The EF of OC is not assessed in their study on paddy-residue

Table 3. Emission budget of carbonaceous species from post-harvest agricultural-waste burning in the Indo-Gangetic Plain (IGP)

Open biomass Paddy-residue burning (October–November)	Emission factor ^a (g/kg)	Fuel load ^b (Kg/sq. km)	Area burnt ^c (sq. km/y)	Emission budget ^d
OC	7.6 ± 1.2	11.8×10^5	48400	436 ± 68 Gg/y
EC	0.72 ± 0.03			41 ± 2 Gg/y
$\Sigma PAHs$	2.8 ± 0.5^e			161 ± 31 Mg/y
Wheat-residue burning (April–May)				
OC	1.2 ± 0.03	5.94×10^5	48400	69 ± 2 Gg/y
EC	0.31 ± 0.02			18 ± 1 Gg/y
$\Sigma PAHs$	0.4 ± 0.1^e			21 ± 6 Mg/y

^aEF modified, after (Kanokkanjana et al., 2011) for paddy-residue burning and, after (Hays et al., 2005) for wheat-residue burning.

^bAdopted from a study in the IGP (Badarinath et al., 2006).

^cInferred from MODIS (Aqua/Terra) satellite data (Resolution: $1^\circ \times 1^\circ$ lat.–long. grid).

^dEmission factor \times fuel load \times area.

^eEmission factor in mg/kg.

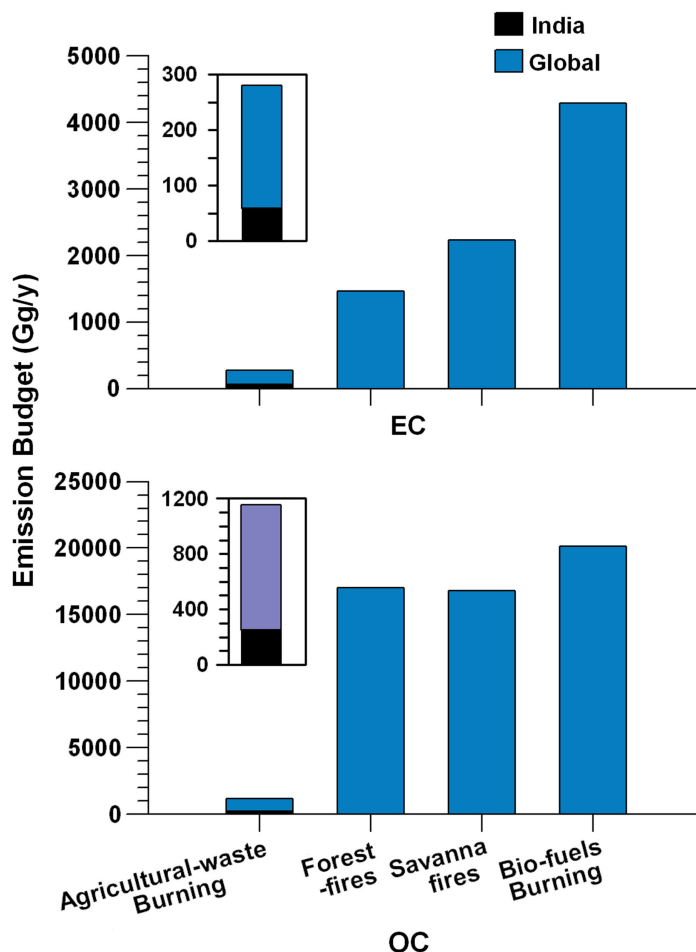


Fig. 5. Emission budgets of aerosol OC (primary) and EC from different biomass burning over the globe. Our data put together with a recent emission inventory suggest that OC and EC produced from agricultural-waste burning in the IGP (Northern India; shown as inset) contributes to $\sim 22\%$ [primary OC: 252 ± 34 Gg/y] and 21% [EC: 59 ± 2 Gg/y], respectively, on the global agricultural-waste burning emission scale.

burning emissions, unlike our approach using the following equation:

$$EF_{OC} (g/kg) = \frac{OC}{EC} * EF_{EC} (g/kg) \quad (2)$$

And, the EF of Σ PAHs for paddy-residue burning is estimated from the mass fraction of PAH (Σ PAHs/OC), using the following equation:

$$EF_{PAHs} (mg/kg) = \frac{\Sigma PAHs (mg)}{OC (g)} * EF_{OC} (g/kg) \quad (3)$$

For wheat-residue burning emissions, the mass fraction of OC ($26 \pm 5\%$) in the IGP is quite similar to that reported from a chamber experiment (Hays et al., 2005). However, the contribution of EC ($6.9 \pm 2.5\%$) in $PM_{2.5}$ from wheat-residue burning emission in the IGP is about 1.6 times lower as compared to 11% in the chamber (Hays et al., 2005). Therefore, we have used the same EF for OC and

scaled down the EF of EC by a factor of 1.6 as reported by (Hays et al., 2005) for wheat-residue burning emission under ambient atmospheric conditions (Table 3). The EF of Σ PAHs for paddy-residue burning is estimated from eq. (3).

The value of fuel load (Table 3) for the paddy- and wheat-residues over the agricultural fields is adopted from a recent literature representing the agricultural-scenario for the states of Punjab in the IGP (Badarinath et al., 2006).

Based on the analysis of open fire-counts satellite data (Resolution: $1^\circ \times 1^\circ$, latitude-longitude grid) from the MODIS (on-board Aqua/Terra; level 2) during 2008–2011, the fire active (agricultural-waste burning) area in the IGP (Fig. 1; including the states of Punjab, Haryana and western part of UP) is estimated to be 48400 sq. km (Justice et al., 2002). The fire-count data (Fig. 1) has been corrected for Cloud and Overpass. The ‘Cloud and Overpass corrected fire-pixel count’ represents the number

of pixels corrected for multiple satellite overpass, missing observations and variable cloud cover (Justice et al., 2002). Since the region (upwind IGP) is fire active for a total of 4 months in a year: due to the practice of paddy-residue burning during October–November and wheat-residue burning during April–May. Therefore, it is considered logical to estimate the emission of aerosols in the IGP from the paddy- and wheat-residue burning only for 2 months each, and represented here as the total emission (Table 3).

3.4. A global scenario on biomass burning emissions

Recently the global emission budget of EC and OC has been revised (Bond et al., 2013). Accordingly, ~ 62 Tg/y of OC (primary) and ~ 14 Tg/y of EC are emitted from the biomass burning and fossil-fuel combustion sources over the globe. Between the two sources, emission from biomass burning is dominant: producing $\sim 89\%$ of the total OC and 60% of the total EC. Furthermore, among the biomass burning sources, the major source of OC (26 Tg/y) and EC (4.3 Tg/y) is the bio-fuel burning (Fig. 5). The emission from savanna fires produces ~ 17 Tg/y of OC and 2.2 Tg/y of EC. The forest fires produce ~ 17 Tg/y of OC and 1.5 Tg/y of EC. The agricultural-waste burning emissions are reported to produce 1154 Gg/y of OC and 280 Gg/y of EC on a global scale. In this context, the net emissions of OC and EC from agricultural-waste burning from the IGP (Northern India) are estimated as 505 ± 68 and 59 ± 2 Gg/y, respectively (Table 3). Using the EC-tracer method (Castro et al., 1999), it has been estimated that $\sim 50\%$ of the OC is primary during both the paddy- and wheat-residue burning emissions. Thus, the net emission of primary OC from agricultural-waste (paddy- and wheat-residue) burning is estimated as 252 ± 34 Gg/y. As far as the emission budgets from the agricultural-waste burning on a global scale are concerned, $\sim 22\%$ of primary OC [252 ± 34 Gg/y] and 21% of EC [59 ± 2 Gg/y] are produced from the IGP (Northern India; Fig. 5). However, on a global biomass burning emission scale, as of present understanding, the contribution of primary OC and EC from the agricultural-waste burning emission is 2 and 3%, respectively (Bond et al., 2013).

4. Conclusions and implications

Large-scale emissions from paddy-residue burning during October–November and wheat-residue burning in April–May are conspicuous features in the IGP. We document significant differences in the OC/EC, nss-K⁺/OC, WSOC/OC, ΣPAHs/EC and PAH isomer ratios for the two biomass burning sources. Relatively high emissions of OC, EC and PAHs are associated with the paddy-residue

burning compared to that from wheat-residue burning emissions. The high abundance of OC, shallow boundary layer height during the wintertime and secondary formation of organic aerosols contribute to the fog and haze conditions over Northern India. This also addresses the issue of over projecting the role of black carbon in the atmospheric radiative forcing over Northern India. The large seasonal variability in aerosol composition associated with varying biomass burning emissions vis-à-vis fossil-fuel combustion sources in the IGP have implications to heterogeneous-phase chemistry of organic aerosols and oxidants (O₃ and OH radical).

5. Acknowledgements

We acknowledge the funding support received from Indian Space Research Organization-Geosphere Biosphere Program Office (Bengaluru, India). We are thankful to Punjab Agricultural University (Dr. Varinderpal Singh) for providing the data on moisture content of post-harvest crop-residues from agricultural fields in Punjab state (in the Indo-Gangetic Plain). We thank two anonymous reviewers for providing their constructive comments and suggestions and Dr. Kaarle Hämeri for editorial handling of the manuscript.

References

- Badarinath, K. V. S., Chand, T. R. K. and Prasad, V. K. 2006. Agricultural crop residue burning in the Indo-Gangetic Plains – a study using IRS-P6 A WiFS satellite data. *Curr. Sci.* **91**, 1085–1089.
- Bari, M. A., Baumbach, G., Kuch, B. and Scheffknecht, G. 2009. Wood smoke as a source of particle-phase organic compounds in residential areas. *Atmos. Environ.* **43**, 4722–4732.
- Birch, M. E. and Cary, R. A. 1996. Elemental carbon-based method for monitoring occupational exposures to particulate diesel exhaust. *Aerosol Sci. Technol.* **25**, 221–241.
- Bond, T. C., Doherty, S. J., Fahey, D. W., Forster, P. M., Berntsen, T. and co-authors. 2013. Bounding the role of black carbon in the climate system: a scientific assessment. *J. Geophys. Res.* DOI: 10.1002/jgrd.50171.
- Castro, L. M., Pio, C. A., Harrison, R. M. and Smith, D. J. T. 1999. Carbonaceous aerosol in urban and rural European atmospheres: estimation of secondary organic carbon concentrations. *Atmos. Environ.* **33**, 2771–2781.
- Decesari, S., Facchini, M. C., Carbone, C., Giulianelli, L., Rinaldi, M. and co-authors. 2010. Chemical composition of PM10 and PM1 at the high-altitude Himalayan station Nepal Climate Observatory-Pyramid (NCO-P) (5079 m a.s.l.). *Atmos. Chem. Phys.* **10**, 4583–4596.
- Gupta, P. K., Sahai, S., Singh, N., Dixit, C. K., Singh, D. P. and co-authors. 2004. Residue burning in rice-wheat cropping system: causes and implications. *Curr. Sci.* **87**, 1713–1717.

- Hays, M. D., Fine, P. M., Geron, C. D., Kleeman, M. J. and Gullett, B. K. 2005. Open burning of agricultural biomass: physical and chemical properties of particle-phase emissions. *Atmos. Environ.* **39**, 6747–6764.
- Justice, C. O., Giglio, L., Korontzi, S., Owens, J., Morissette, J. T. and co-authors. A. 2002. The MODIS fire products. *Remote Sens. Environ.* **83**, 244–262.
- Kanokkanjana, K., Cheewaphongphan, P. and Garivait, S. 2011. Black carbon emission from paddy field open burning in Thailand. *IPCBE Proc.* **6**, 88–92.
- Keene, W. C., Pszenny, A. A. P., Galloway, J. N. and Hawley, M. E. 1986. Sea-salt corrections and interpretation of constituent ratios in marine precipitation. *J. Geophys. Res.* **91**, 6647–6658.
- Khalili, N. R., Scheff, P. A. and Holsen, T. M. 1995. PAH source fingerprints for coke ovens, diesel and, gasoline engines, highway tunnels, and wood combustion emissions. *Atmos. Environ.* **29**, 533–542.
- Khillare, P., Balachandran, S. and Hoque, R. 2005a. Profile of PAH in the exhaust of gasoline driven vehicles in Delhi. *Environ. Monit. Assess.* **110**, 217–225.
- Khillare, P. S., Balachandran, S. and Hoque, R. R. 2005b. Profile of PAHs in the diesel vehicle exhaust in Delhi. *Environ. Monit. Assess.* **105**, 411–417.
- Kirton, P. J., Ellis, J. and Crisp, P. T. 1991. The analysis of organic matter in coke oven emissions. *Fuel*. **70**, 1383–1389.
- Li, P.-h., Wang, Y., Li, Y.-H., Wang, Z.-F., Zhang, H.-Y. and co-authors. 2010. Characterization of polycyclic aromatic hydrocarbons deposition in PM_{2.5} and cloud/fog water at Mount Taishan (China). *Atmos. Environ.* **44**, 1996–2003.
- Lim, H. J., Turpin, B. J., Russell, L. M. and Bates, T. S. 2003. Organic and elemental carbon measurements during ACE-Asia suggest a longer atmospheric lifetime for elemental carbon. *Environ. Sci. Technol.* **37**, 3055–3061.
- Masclat, P., Cachier, H., Liousse, C. and Wortham, H. 1995. Emissions of polycyclic aromatic hydrocarbons by savanna fires. *J. Atmos. Chem.* **22**, 41–54.
- Mayol-Bracero, O. L., Guyon, P., Graham, B., Roberts, G., Andreae, M. O. and co-authors. 2002. Water-soluble organic compounds in biomass burning aerosols over Amazonia 2. Apportionment of the chemical composition and importance of the polyacidic fraction. *J. Geophys. Res.* **107**, 8091.
- Pavuluri, C. M., Kawamura, K., Aggarwal, S. G. and Swaminathan, T. 2011. Characteristics, seasonality and sources of carbonaceous and ionic components in the tropical aerosols from Indian region. *Atmos. Chem. Phys.* **11**, 8215–8230.
- Pöhlker, C., Wiedemann, K. T., Sinha, B., Shiraiwa, M., Gunthe, S. S. and co-authors. 2012. Biogenic potassium salt particles as seeds for secondary organic aerosol in the Amazon. *Science*. **337**, 1075–1078.
- Punia, M., Nautiyal, V. P. and Kant, Y. 2008. Identifying biomass burned patches of agricultural residue using satellite remote sensing data. *Curr. Sci.* **94**, 1185–1190.
- Rajput, N. and Lakhani, A. 2008. Measurements of polycyclic aromatic hydrocarbons at an industrial site in India. *Environ. Monit. Assess.* **150**, 273–284.
- Rajput, P., Sarin, M. M. and Kundu, S. S. 2013. Atmospheric particulate matter (PM_{2.5}), EC, OC, WSOC and PAHs from NE-Himalaya: abundances and chemical characteristics. *Atmos. Poll. Res.* **4**, 214–221.
- Rajput, P., Sarin, M. M. and Rengarajan, R. 2011a. High-precision GC-MS analysis of atmospheric polycyclic aromatic hydrocarbons (PAHs) and isomer ratios from biomass burning emissions. *J. Environ. Prot.* **2**, 445–453.
- Rajput, P., Sarin, M. M., Rengarajan, R. and Singh, D. 2011b. Atmospheric polycyclic aromatic hydrocarbons (PAHs) from post-harvest biomass burning emissions in the Indo-Gangetic Plain: isomer ratios and temporal trends. *Atmos. Environ.* **45**, 6732–6740.
- Ram, K. and Sarin, M. M. 2010. Spatio-temporal variability in atmospheric abundances of EC, OC and WSOC over Northern India. *J. Aerosol Sci.* **41**, 88–98.
- Ram, K. and Sarin, M. M. 2011. Day-night variability of EC, OC, WSOC and inorganic ions in urban environment of Indo-Gangetic Plain: implications to secondary aerosol formation. *Atmos. Environ.* **45**, 460–468.
- Ram, K., Sarin, M. M. and Hegde, P. 2010. Long-term record of aerosol optical properties and chemical composition from a high-altitude site (Manora Peak) in Central Himalaya. *Atmos. Chem. Phys.* **10**, 11791–11803.
- Ram, K., Sarin, M. M. and Tripathi, S. N. 2012. Temporal trends in atmospheric PM_{2.5}, PM₁₀, elemental carbon, organic carbon, water-soluble organic carbon, and optical properties: impact of biomass burning emissions in the Indo-Gangetic Plain. *Environ. Sci. Technol.* **46**, 686–695.
- Ramanathan, V., Li, F., Ramana, M. V., Praveen, P. S., Kim, D. and co-authors. 2007. Atmospheric brown clouds: hemispherical and regional variations in long-range transport, absorption, and radiative forcing. *J. Geophys. Res.* **112**, D22S21.
- Rengarajan, R., Sarin, M. M. and Sudheer, A. K. 2007. Carbonaceous and inorganic species in atmospheric aerosols during wintertime over urban and high-altitude sites in North India. *J. Geophys. Res.* **112**, D21307.
- Schauer, J. J., Kleeman, M. J., Cass, G. R. and Simoneit, B. R. T. 2001. Measurement of emissions from air pollution sources. 3. C₁ – C₂₉ organic compounds from fireplace combustion of wood. *Environ. Sci. Technol.* **35**, 1716–1728.
- Sharma, H., Jain, V. and Khan, Z. 2008. Atmospheric polycyclic aromatic hydrocarbons (PAHs) in the urban air of Delhi during 2003. *Environ. Monit. Assess.* **147**, 43–55.
- Sheesley, R. J., Schauer, J. J., Chowdhury, Z., Cass, G. R. and Simoneit, B. R. T. 2003. Characterization of organic aerosols emitted from the combustion of biomass indigenous to South Asia. *J. Geophys. Res.* **108**, 4285.
- Srinivas, B., Kumar, A., Sarin, M. M. and Sudheer, A. K. 2011. Impact of continental outflow on chemistry of atmospheric aerosols over tropical Bay of Bengal. *Atmos. Chem. Phys. Discuss.* **11**, 20667–20711.
- Venkataraman, C., Reddy, C. K., Josson, S. and Reddy, M. S. 2002. Aerosol size and chemical characteristics at Mumbai, India, during the INDOEX-IFP (1999). *Atmos. Environ.* **36**, 1979–1991.